

UC San Diego

UC San Diego Electronic Theses and Dissertations

Title

The Regulation of Toll-signaling by the Sbf complex in D. Melanogaster

Permalink

<https://escholarship.org/uc/item/23b06763>

Author

Saluja, Abhishek

Publication Date

2013

Peer reviewed|Thesis/dissertation

UNIVERSITY OF CALIFORNIA, SAN DIEGO

The Regulation of Toll-signaling by the Sbf complex in *D. Melanogaster*

A Thesis submitted in partial satisfaction of the requirements for the degree of Master of Science

in

Biology

by

Abhishek Saluja

Committee in charge:

Professor Amy Kiger, Chair
Professor Steven A. Wasserman
Professor James E. Wilhelm

2013

The Thesis of Abhishek Saluja is approved and it is acceptable in quality and form for publication on microfilm and electronically:

Chair

University of California, San Diego

2013

TABLE OF CONTENTS

Signature Page.....	iii
Table of Contents.....	iv
List of Figures.....	v
Abstract of the Thesis.....	vi
Introduction.....	1
Results.....	5
Discussion.....	20
Materials and Methods.....	25
References.....	29

LIST OF FIGURES

Figure 1:	Pi3K68D and Sbf genetically interact with hyper-activated Toll-induced melanotic masses.....	13
Figure 2:	Toll localization is shifted when Pi3K68D or Sbf is over-expressed.....	14
Figure 3:	Toll receptor internalization requires the MTM “pseudo”-phosphatase Sbf....	15
Figure 4:	Toll protein levels did not change as Pi3K68D, Sbf, or Rab21 were knocked down.....	16
Figure 5:	Knockdown of Sbf but not Pi3K68D blocks internalization of Toll in fat body.	17
Figure 6:	Cactus protein levels decrease after 30 minutes.....	18
Figure 7:	Depletion of Atg1 suppresses the number and presence of melanotic masses.....	19

ABSTRACT OF THE THESIS

The Regulation of Toll-Signaling by the Sbf Complex in *D. Melanogaster*

by

Abhishek Saluja

Master of Science in Biology

University of California, San Diego, 2013

Professor Amy Kiger, Chair

Membrane trafficking is the process of intracellular transport of cargo in vesicles. Cells are highly compartmentalized, and thus regulate necessary functions through trafficking. Phosphoinositides and Rab GTPases are important components that are trafficked. Our lab has identified a phosphoinositide and Rab GTPase co-regulatory complex called the Sbf complex. The Sbf complex has specific functions in endosomal trafficking. The Toll-signaling pathway is known to induce the formation of melanotic masses (tumors) upon hyper-activation. The

discovery of masses in fly macrophages (hemocytes) while studying the Sbf complex led me to study the impact of modulating the Sbf complex on Toll-signaling, with the goal of identifying mechanisms of Sbf complex function. I show here that over-expression and loss of function of the Sbf complex led to mass suppression in third instar *Drosophila* larvae. While the Toll protein levels were unchanged with loss of function of the Sbf complex, the endocytosis of Toll differed in each condition. The level of Toll endocytosis was different when individual members of the Sbf complex were depleted. This difference in endocytosis of Toll is shown in both hemocytes and fat body (liver). In addition, our lab has shown that the Sbf complex is required for proper autophagosome trafficking, a key step in autophagy, the process of degrading cytoplasmic materials in the lysosome. Here I also show how depletion of a key autophagic gene led to mass suppression. This indicated the potential impact of autophagy on the Toll-signaling pathway. These studies suggest that the impact of the Sbf complex on Toll-signaling could be at the level of Toll endocytosis and/or an autophagy-dependent response. In addition to understanding mechanisms of Sbf complex functions, these findings show that key steps of the autophagic process could potentially be necessary for the signal to be fully transduced along the Toll-signaling pathway.

INTRODUCTION

Membrane trafficking is defined as the transport of cargo through vesicles. Internalization of a receptor at the plasma membrane and its subsequent sorting is an example of membrane trafficking. Endocytosis describes the engulfment of components such as plasma membrane receptors from the plasma membrane to intracellular vesicles. Once internalized, trafficking of the receptor occurs along a determined pathway. Research links defects in endosomal trafficking with disorders such as Hermansky-Pudlak syndrome, Danon disease, Charcot-Marie-Tooth type 2 Neuropathy, X-linked mental retardation, tuberous sclerosis, and Stiff-Mann syndrome (Puertollano, 2006). Thus, understanding the mechanisms that regulate endocytosis and the subsequent trafficking pathways has great importance to human health.

Once internalized, plasma membrane receptors are found on endocytic vesicles that will fuse to form early endosomes (Lodish et al. 2000). This endosomal vesicle is given identity by endosomal markers present on the vesicular membrane such as lipids and Rab GTPases (Russell et al. 2006). The endocytosed cargo is trafficked through the endocytic pathway from early endosomes to late endosomes (Vanlandingham et al. 2009). Furthermore, this allows for the cargo to be delivered to the lysosomes (Luzio et al, 2009). The cargo delivered to the lysosome is degraded in this acidic compartment (Kolter et al. 2010). A phosphoinositide and Rab regulatory complex, called the Sbf complex, plays a key role in regulation of endosomal trafficking (Jean et al. 2012), and thus provides an important example in understanding the different outcomes that result from cargo trafficking.

Sbf is catalytically inactive and is thereby classified as a MTM pseudo-phosphatase. Sbf interacts as a scaffold for the catalytic phosphatase Mtm and with the Class-II-P(I)3-kinase Pi3K68D. This promotes coordinated regulation of a P(I)3P pool that is essential for endosomal

trafficking (Jean et al. 2012). Sbf is also a guanine exchange factor (GEF) for Rab21. Thus, Sbf coordinates Pi3P and Rab21 regulation within the endosomal pathway.

While studying Sbf, Rab21, Pi3K68D, and Mtm interactions, our lab found that loss of function of *Rab21* causes the formation of melanotic masses. Masses arise when hemocytes mediate an immune response (Qui et al. 1998) that leads to aggregation of cells, phagocytosis of cells, or an induction of the melanization cascade (Meister et al. 2003). The masses have been shown to arise from hyper-activation of different pathways, including Toll (Minakhina et al. 2006). Toll gain of function or cactus loss of function mutations lead to proliferation of hemocytes and production of melanotic masses (Minakhina et al. 2006). Along with *Rab21* loss of function, the Toll^{10B} constitutively active point mutation leads to masses (Qiu et al. 1998). This effect can be replicated by targeted expression of a UAS-driven Toll^{10B}:GFP in hemocytes (Tanji et al. 2007). In addition, constitutive activation of the Jak/Stat pathway in the Hop^{Tum} mutant produces similar phenotypes (Minakhina et al. 2006).

The Toll receptor is also activated by a gram positive and (in flies) fungal infection (Lemaitre et al. 1996; Michel et al. 2001; Fujita et al. 2011 and Bettencourt et al. 2004). Significantly, endocytosis of Toll is also required for an appropriate innate immune response (Huang et al. 2010). The fact that there is co-localization between the fly Toll receptor and Rab5 (Lund et al., 2010), and that endocytosis of Toll is required for signaling, signifies the importance of studying the signaling pathway and the trafficking of Toll for better understanding immunity.

The Toll pathway was originally understood/discovered through its function in embryonic patterning where upon fertilization the Spätzle ligand triggers Toll activity (Anderson 1998) and ultimately nuclear translocation of the Dorsal transcription factor (Reichhart et al. 1993). Dorsal/ventral axis formation in *Drosophila* relies on Toll (Anderson et al. 1985). This occurs on the ventral side of the embryo, and thus, a gradient is formed (Rushlow et al. 1989; and Roth et

al. 1989). The gradient causes the formation of a dorsal/ventral axis (Steward 1989). Importantly, dorsal/ventral formation was shown to depend on endocytosis (Lund et al. 2010). Dynasore is an inhibitor of dynamin (Masia et al. 2006). Addition of Dynasore led to disruption of dynamin, which is an essential regulator of endocytosis (McNiven, 1998; and Sever 2002). This led to a decrease in nuclear dorsal levels and D/V patterning defects (Lund et al 2010). This is an indication that endocytosis is required for signaling. In addition to forming the dorsal/ventral axis, this nuclear translocation of the transcription factor Dif/Dorsal is the mechanism that produces anti-microbial peptides to fight a gram-positive infection (Valanne et al. 2011).

Toll has been shown to interact with the endosomal proteins Myopic (Mop), and with the hepatocyte growth factor-regulated tyrosine kinase substrate (Hrs). Mop and Hrs are shown to be required for the activation of the Toll-signaling pathway. These two are important members of the ESCRT-0 endocytosis complex, and have been shown to co-localize with the Toll receptor at endosomes (Huang et al. 2010).

Given the similar phenotypes between *Rab21* loss of function and Toll^{10B}:GFP over-expression, I examined the trafficking of the Toll receptor and transduction of the signal in the fruit fly. Preliminary results suggested that the Toll pathway could be improperly regulated in larvae depleted of Sbf complex members. Thus, I hypothesize that the Sbf complex's role in endocytosis regulates Toll function, perhaps through trafficking of Toll receptor. To test this I tested genetic interactions at the level of Toll signaling response, which included melanotic mass formation, or transduction of the signal. In addition, I tested the Toll receptor distribution and trafficking. I tested whether over-expression or loss of function of *Pi3K68D*, *Sbf*, or *Rab21*, while co-expressed with a hyper-activated Toll-signaling pathway, would attenuate the signaling pathway and impact the production of melanotic masses. Here I present evidence that indeed, Sbf complex members regulate Toll.

In *Drosophila Melanogaster* (fruit fly), the Toll-signaling pathway is well characterized (Silverman et al. 2009). Therefore, the system provides an ideal genetic system to study its regulation. The Gal4/UAS system allows for inducible tissue specific gene expression (Osterwalder et al. 2001). Additionally, the life cycle of the fruit fly spans a short time. While the fruit fly hemocyte is a macrophage-equivalent (Williams 2007), the fruit fly fat body is a liver equivalent (Abel et al. 1992; and Sondergaard 1993). Both hemocytes and fat body express the Toll receptor and mediate immune responses to Toll signaling. Furthermore, fruit fly S2R+ cells are hemocyte-derived cells that are used for studies in *Drosophila* (Yanagawa et al. 1998). Thus, these allow for multiple cell types for the study of Toll signaling.

RESULTS

Pi3K68D and Sbf genetically interact with hyper-activated Toll-induced melanotic masses

Our lab previously showed that *Rab21* depletion led to melanotic masses in third instar larvae. Sbf interacts with Pi3K68D, Mtm and Rab21 to promote PI(3)P homeostasis, Rab21 activation and endosomal traffic (Jean et al. 2012). Toll^{10B}, a point mutant that leads to hyper-activation (Hu et al. 2004) in the absence of the Spätzle ligand (Tanji et al. 2007), was shown previously to induce melanotic masses (Minakhina et al. 2006). Toll relies on endocytosis (Lund et al. 2010) and trafficking for signaling (Belvin et al. 1996). Given that *Rab21* loss of function causes a similar phenotype of melanotic masses, I hypothesized that Sbf complex functions may normally act to downregulate Toll signaling. Fusion proteins of Toll or Toll^{10B} tagged with green fluorescent protein (Toll:GFP, Toll^{10B}:GFP) allows for targeted overexpression and localization of the Toll protein to be studied. To test my hypothesis, I co-expressed Toll^{10B} with either overexpression or RNAi alleles of Sbf complex genes in hemocytes. I predicted that a change in the level of *Sbf*, *Pi3K68D*, or *Rab21* (hereafter referred to as the Sbf complex) would affect the Toll-signaling pathway and impact the production of melanotic masses.

If Sbf complex downregulates Toll activity then overexpression of Sbf may suppress Toll^{10B} activation of masses. Co-expression of *Pi3K68D* or *Sbf*, in the presence of a hyper-activated Toll receptor (through the use of Toll^{10B}:GFP) led to suppression of the average number of melanotic masses per larvae (Fig1A, 1B, 1C, and 1H), as compared to Toll^{10B}:GFP alone (Fig 1H). Co-expression also suppressed the percentage of larvae that displayed melanotic masses (Fig1A, 1B, 1C, and 1G), consistent with Sbf complex function antagonistic to Toll. Conversely, I predicted that if Sbf complex normally downregulates Toll activity, then Sbf complex depletion should lead to further Toll activation. However, loss of function of *Pi3K68D* or *Sbf* also led to suppression of the average number of masses per larvae (Fig 1D, and 1H), but not the

percentage of Toll^{10B} larvae with masses (Fig 1D, and 1G). The combination of Toll^{10B} with *Rab21* loss of function severely hindered the larval progression from 2nd instar to 3rd instar stage. The larvae were extremely sick, and displayed a plethora of melanotic masses even at the 2nd instar stage. Therefore, the impact of *Rab21* on melanotic masses was experimented in non hyper-activated conditions with wild type Toll:GFP (Fig 1I). The presence of masses persisted in this condition (Fig 1J). In addition to the difference that Toll wildtype was overexpressed, the incubation temperature was decreased from 29° C to 25° C. This decrease in temperature affects the temperature sensitivity of the GAL4/UAS response. Due to the lack of 3rd instar larvae upon depletion of *Rab21* I was unable to further delineate the GTPase's function in Toll-signaling. Overall these results indicate that the ability of Toll to induce melanotic masses was attenuated by overexpression or knockdown of the Sbf complex.

Toll localization is shifted when Pi3K68D or Sbf is overexpressed

Since Toll requires endocytosis and trafficking for maximal signaling, I examined the distribution and localization of the Toll receptor together with Sbf Complex gain or loss of function. Following activation, Toll is endocytosed and localizes to the early endosomal complex (Huang et. al 2010). Overexpressed Toll:GFP and Toll^{10B}:GFP display different localization patterns in macrophages. Toll^{10B} is mostly found intracellularly, presumably due to its activated state.

To address whether Sbf complex function affects Toll receptor localization, I first asked whether distribution of Toll was altered with increased levels of either *Pi3K68D* or *Sbf*. Toll localization was classified into four distinct categories: external, internal, internal vesicle, or diffused. Toll:GFP localizes mostly along the plasma membrane, classified here as “external” (Fig 2B, and 2H). When *Pi3K68D* was co-expressed, Toll shifted internally into rings, or “internal vesicles” (Fig 2C, and 2H). This shift was also observed when *Sbf* is co-expressed (Fig 2D, and 2H). In contrast to wildtype Toll:GFP, Toll^{10B}:GFP is found internally (Fig 2E, and 2I). When

Pi3K68D or *Sbf* were co-expressed, Toll remained internal (Fig 2F, and 2I). Although no shift in Toll^{10B}:GFP internal localization was observed, it is possible that an undetected compartmental shift occurred. The shift in Toll:GFP localization from the plasma membrane is consistent with a possible role for the Sbf complex in endosomal trafficking.

Toll receptor internalization requires the MTM “pseudo”-phosphatase Sbf

To address the question of whether Toll receptor endocytosis is affected by the Sbf complex, I analyzed the amount of Toll receptor being internalized into the cell. Internalization of the activated Toll receptor is necessary for full activation of the Toll-signaling pathway (Huang et al. 2010). Since the Sbf Complex interacts with a role in endosomal trafficking (Jean et al. 2012) and overexpression of either promoted Toll:GFP internal localization (above), I hypothesized that Toll receptor endocytosis or trafficking may be affected in *Pi3K68D* or *Sbf* loss of function conditions. Internalization of the Toll receptor was analyzed using an antibody uptake assay, in which hemocytes were incubated with an antibody against the extracellular portion of Toll, then permitted to undergo internalization for 15 minutes prior to a two-step staining procedure. The experiment was done in a Toll:GFP background because of the weak signal found in wild type. Toll internalization was observed through an increase in the intensity of internalized surface-labeled receptor after 15 minutes (Fig 3A, and 3D). When *Pi3K68D* was knocked down, the intensity of internalized Toll antibody increased similar to control (Fig 3B, and 3D). However, *Sbf* depletion blocked the increase in the intensity of internalized antibody (Fig 3C, and 3D).

This data suggests that internalization of the Toll receptor occurs in hemocytes. Loss of function of *Pi3K68D* did not affect internalization of Toll, while loss of function of *Sbf* blocked Toll uptake. Therefore, *Sbf* may have an essential role in Toll endocytosis. This led me to question if Toll receptor localization or protein levels varied when Sbf complex components were knocked down.

Toll protein levels did not change with Pi3K68D, Sbf, or Rab21 knockdown.

Knockdown of *Pi3K68D* in the *Drosophila* hemocytes did not block endocytosis of the Toll receptor, while knockdown of *Sbf* did. Whether this difference between endocytosis of Toll during loss of function of *Pi3K68D* and *Sbf* was because of a difference in the amount of Toll protein due to degradation or recycling was unclear. Endocytosed cargo is eventually delivered to the lysosomes (Luzio et al, 2009) and this cargo is degraded in this acidic compartment (Kolter et al. 2010). Toll protein levels may differ when either *Pi3K68D* or *Sbf* is knocked down if there is an alteration in Toll protein degradation. Additionally, if there is an inhibition in the amount of Toll being internalized, the amount of Toll participating in the Toll-signaling pathway may differ within each respective condition. Therefore, I hypothesized that the amount of Toll protein may differ between *Pi3K68D* and *Sbf* loss of function potentially due to the lack of recycling, or change in degradation.

Confocal microscopy of the knockdown conditions was performed in hemocytes. As compared to Toll:GFP along the plasma membrane in control cells, Toll:GFP showed a predominantly internal localization in *Pi3K68D* or *Sbf* knockdown conditions (Fig 4A), and similarly internal in overexpression conditions (Fig 2B, 2C, and 2D). In addition, endogenous Toll protein level was monitored by immunoblots. S2R+ fly cells, a hemocyte like cell culture line, were subjected to RNAi. With S2R+ usage, the quantity of cells in study is higher, and the RNAi is easily administered. All Sbf complex members were efficiently knocked down in S2R+ cells (Fig 4B). GFP RNAi served as the negative control. Quantification of endogenous Toll protein levels showed no significant decrease in any RNAi conditions, except when *Toll* itself was knocked down (Fig 4C). These results show that, although Toll localization was affected in hemocytes, Toll protein levels were unaffected by Sbf complex member knockdown in S2R+ cells.

Knockdown of *Sbf* but not *Pi3K68D* blocked internalization of stimulated Toll in fat body.

The fat body in *D. Melanogaster* is analogous to the liver in mammals (Abel et al. 1992). Importantly, addition of gram-positive bacterial component peptidoglycan (PGN) has been shown to induce the Toll-signaling pathway in fat bodies dissected from third instar larvae (Bettencourt et al, 2004). Therefore, PGN addition gave me the opportunity to study Toll internalization following stimulation.

Using a similar uptake assay as above, Toll internalization was studied at 0 and 30 minutes following PGN addition. Control cells showed a significant increase in Toll internalization between times 0 and 30 (Fig 5A, 5B). Toll internalization occurred similarly when *Pi3K68D* was depleted as in the control condition (Fig5A, 5B). Significantly, *Sbf* knockdown decreased Toll internalization compared to control (Fig 5A, 5B). Control cells with no PGN addition showed an insignificant increase in internal Toll at 30 minutes of stimulation.

The internalization results in the fat body indicate that knockdown of *Sbf* but not *Pi3K68D* inhibits internalization of Toll. These results are similar to uptake results obtained in hemocytes (Fig 3) and suggest an important role for *Sbf* in Toll endocytosis.

PGN addition did not affect Cactus protein levels

Addition of gram-positive bacterial component peptidoglycan (PGN) has been shown to induce the Toll-signaling pathway in fat bodies dissected from third instar *Drosophila* larvae (Bettencourt et al. 2004). Pathogen induction of the Toll pathway is well established, and upon PGN addition, the Spätzle ligand is matured. The downstream signal causes Dif/Dorsal to translocate to the nucleus (Lemaitre et al. 1995). However, as the mature ligand binds the Toll receptor, multiple vital adaptor proteins transduce the signal downstream. The MyD88/Tube

membrane associated complex is responsible for recruiting the serine/threonine kinase, Pelle (Belvin et al. 1996, and Sun et al. 2004). Pelle is autophosphorylated, and this phosphorylation is increased in the Toll mutant, Toll^{10B} (Shen et al. 2002). Cactus functions in sequestering Dorsal transcription factor in the cytoplasm, but when the Toll pathway activated, Cactus is degraded (Nicolas et al. 1998) and Dorsal trans-locates to the nucleus (Lemaitre et al. 1995; Manfrulli et al. 1999; Reichhart et al. 1993; Wu et al. 1998; and Whalen et al. 1993). The transcription factor binds its target genes, allowing for anti-microbial peptides (AMPs) to be produced in the fat body (Meister et al. 1997). Thus, the presence of Cactus protein serves as an indicator of the level of activation of the Toll-signaling pathway. Additionally, lipopolysaccharide (LPS) addition has been shown to successfully induce the TLR4 pathway in mouse macrophages (Fujita et al. 2011).

Upon PGN addition to fat body, I found that the level of Cactus protein was unaffected. Although there was an expected decrease in Cactus at 30 minutes after PGN addition in control and *Pi3K68D* loss of function (Fig 6A), the decrease was not significant (Fig 6B). The decrease at 0 and 30 minutes of PGN addition was significant in *Sbf* loss of function (Fig 6A, 6B). However, when no PGN was added there was also a significant decrease in Cactus protein level (Fig 6A, 6B). This indicates that PGN addition is not causing Cactus protein levels to decrease. Therefore, PGN is not serving as an inducer of Toll signaling through Cactus, as hypothesized. To address Toll activity, the PGN treatment method needs to be better controlled to optimize the protocol, or alternatively, an alternate inducer or alternate read-out of activity needs to be utilized.

Depletion of Atg1 suppresses the number and presence of melanotic masses

The process of macro-autophagy involves cytoplasmic materials being degraded in lysosomes during stress (Eskelinen et al. 2009). When nutrients and cellular building blocks are required, the cell uses autophagy to cope with this necessity (Takeshige et al. 1992). Our lab has previously shown *Sbf*, *Rab21* and *Pi3K68D* involvements in autophagy, where they play essential

roles in autophagic flux. Therefore, since Sbf and Pi3K68D are required for autophagy, it is plausible that their requirement for Toll-induced melanotic mass formation depends on autophagy.

To test whether autophagy is required for melanotic mass formation, I tested important autophagic genes known to be functional at different stages of autophagy for interactions with *Toll*^{10B}. *Atg1*, *Atg6*, and *Vps34* loss of function were tested. Knockdown of these genes individually allowed me to delineate whether the gene was essential for Toll^{10B}-induced melanotic masses. Depletion of *Atg1* caused a significant suppression in the average number of masses per larvae (Fig 7D, and 7F). In addition, knockdown of *Atg1* led to a suppression of the percentage of larvae with masses (Fig 7G). *Atg6* knockdown did not suppress the average number of masses per larvae (Fig 7E, 7F, and 7G), although level of knockdown has not been assessed. Inhibition of *Vps34* through RNAi, but not through expression of a dominant negative, led to suppression in the average number of masses present per larvae (Fig 7B, 7C, and 7F). However, the percentage of larvae with masses was not suppressed in either RNAi or dominant negative condition (Fig 7G). From previous studies in the lab, it was shown that the Sbf complex is involved in autophagy, and the results presented here show that autophagy also plays a role in the formation of melanotic masses.

Perspectives

Alternative pathway may cause melanotic masses

Loss of function of *Rab21* causes melanotic masses. Among the known pathways that can induce melanotic masses upon hyper-activation are the Toll, Jak/Stat and Ras/MAPK pathways (Minakhina et al. 2006). A previous finding of our lab showed that depletion of *Sbf*, *Rab21* or *Pi3K68D* did not lead to an increase in the number of hemocytes. This eliminates the Ras/MAPK pathway as a very likely pathway to Sbf complex-mediated mass formation. To explore whether the Sbf complex can genetically interact with the Jak/Stat pathway, I developed a line overexpressing dominant alleles of Jak. I will test the knockdown of *Pi3K68D* or *Sbf* co-expressed with the constitutively activated Jak, Hop-TumL. The melanotic masses will be quantified to determine if *Pi3K68D* or *Sbf* knockdown leads to suppression of the melanotic masses. The overall goal is to determine if Sbf, Pi3K68D, and Rab21 has a broad influence on hemocyte signaling that includes both Toll and Jak/Stat function.

Figures

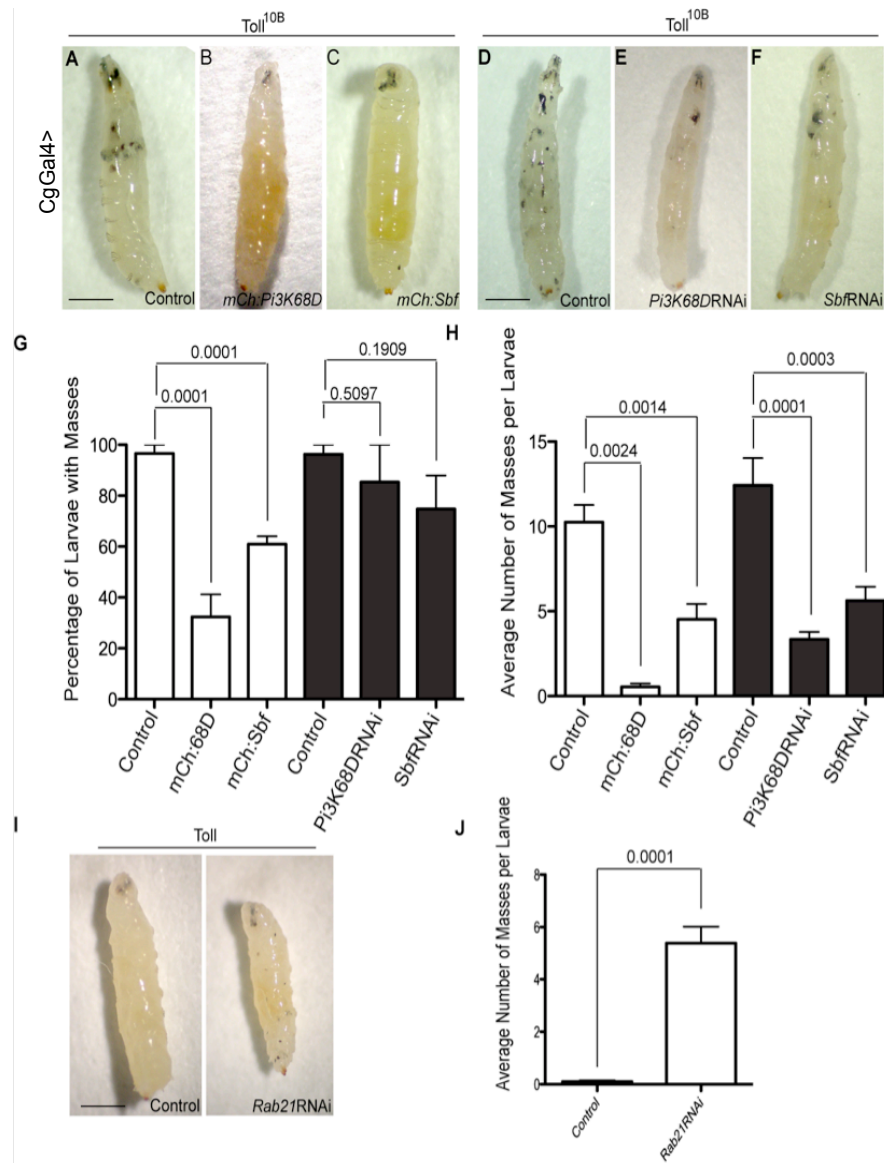


Figure 1: Pi3K68D and Sbf genetically interact with hyper-activated Toll-induced melanotic masses. (A-F) *Drosophila* third instar larvae showing melanotic masses in different conditions. (A) Control image, over-expression of Toll^{10B} induces melanotic masses (dark specks). The CgGal4 driver restricted expression to hemocytes and fat body. (B) Coexpression of the kinase *Pi3K68D*, (C) and the MTM “pseudo”-phosphatase *Sbf*, suppresses Toll^{10B} dependent melanotic masses. (D) Control image, over-expression of Toll^{10B} induces melanotic masses. (E) Knockdown of *Pi3K68D*, (F) or *Sbf* suppresses the number of Toll^{10B} dependent melanotic masses. (G) Percentage of larvae with >1 masses per larvae, +SEM. (H) Average number of masses per larvae, +SEM. (I) When *Rab21* is knocked down melanotic masses result. (J) Average number of masses per larvae, +SEM. The data is representative of three independent experiments. Bars 5µm.

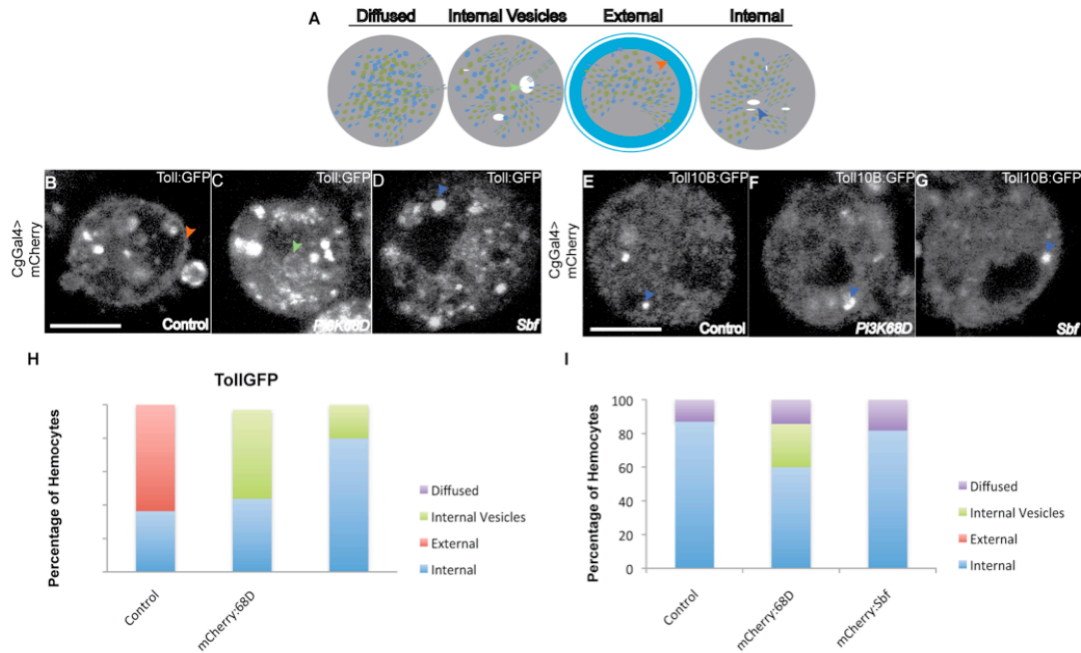


Figure 2: Toll localization is shifted when Pi3K68D or Sbf is over-expressed. (A) Schematic representation. Diffused, Internal Vesicles, External, Internal. (B) Control hemocyte with external localization (red arrowhead). (C) Coexpression of Pi3K68D, with internal vesicle localization (green arrowhead). (D) Coexpression of Sbf, with internal localization (blue arrowhead). (E) Control hemocyte with internal localization (blue arrowhead). (F) Coexpression of Pi3K68D with internal localization (blue arrowhead). (G) Coexpression of Sbf with internal localization (blue arrowhead). (H and I) Distribution of receptor localization in individual hemocytes is quantified as a percentage. (H) Distribution of Toll:GFP. (I) Distribution of Toll^{10B}:GFP. Bars 5µm.

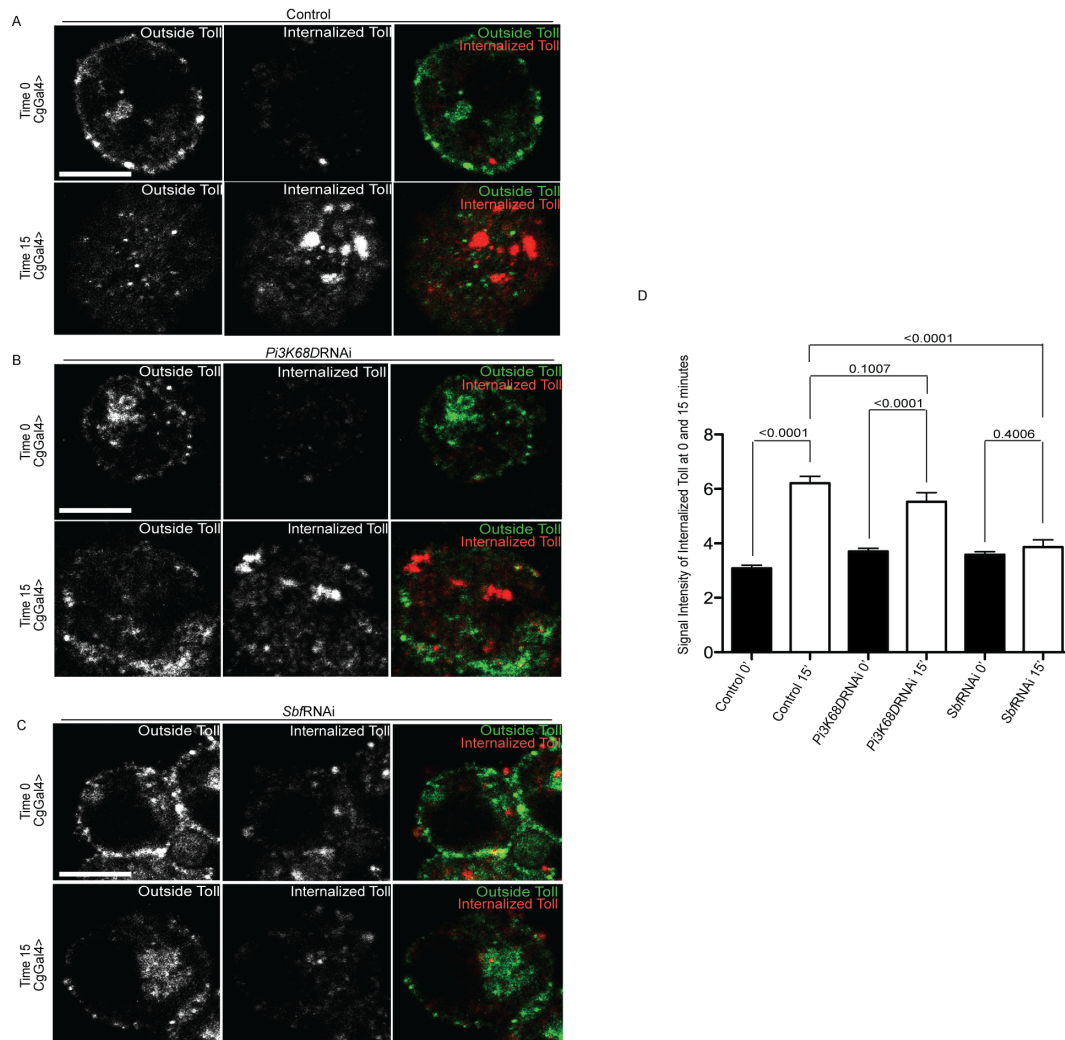


Figure 3: Toll receptor internalization requires the MTM “pseudo”-phosphatase Sbf. (A) Control *Drosophila* third instar larvae showing Toll receptor localization at 0 (upper row) and 15 minutes (lower row). The CgGal4 driver restricted expression to hemocytes and fat body. 3.7% para-formaldehyde used as fixative. (B) *Pi3K68D* RNAi. (C) *Sbf* RNAi. (D) Change in internal intensity measured at 0 and 15 minutes. Change is significant in control and *Pi3K68D* RNAi conditions. Change is insignificant in *Sbf* RNAi. This indicates a block in uptake of the toll receptor, +SEM. The data is representative of three independent experiments. Bars 5 μ m.

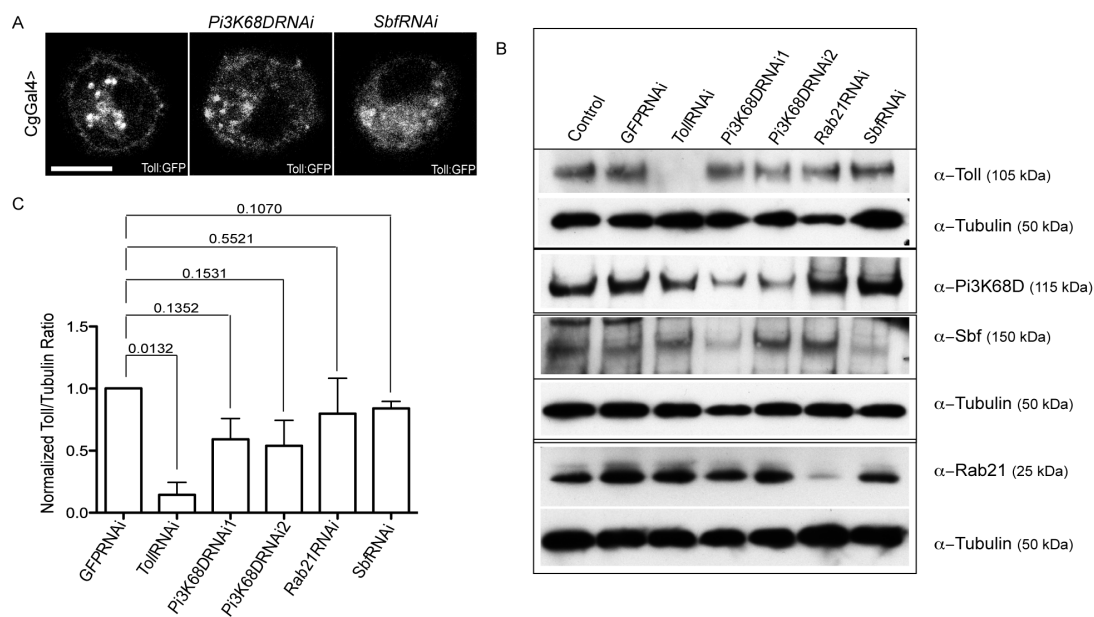


Figure 4: Toll protein levels did not change as Pi3K68D, Sbf, or Rab21 were knocked down. (A) Confocal images of *Drosophila* third instar larvae showing Toll receptor localization in control *Pi3K68D* RNAi or *Sbf* RNAi. (B) Successful knockdown of Toll, Pi3K68D, Sbf, and Rab21 is shown. Tubulin levels show protein loading. (C) Toll protein levels in each lane of the first panel in B are quantified. Normalized

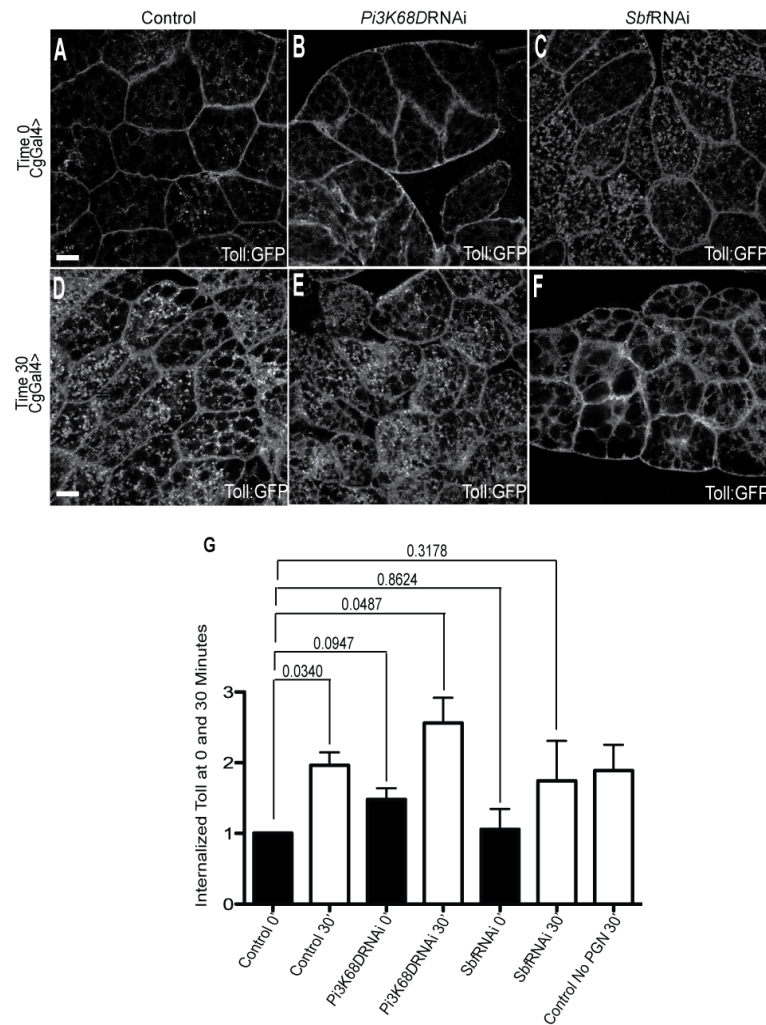


Figure 5: Knockdown of *Sbf* but not *Pi3K68D* blocks internalization of Toll in fat body. (A) Confocal images of *Drosophila* third instar larvae showing Toll receptor localization in control (B) *Pi3K68D* RNAi (C) and *Sbf* RNAi at time 0. (D) Toll receptor localization in control (E) *Pi3K68D* RNAi (F) and *Sbf* RNAi at time 30. (G) Change in internalized Toll at 0 and 30 minutes. Change is significant in control and *Pi3K68D* RNAi conditions. Change is insignificant in *Sbf* RNAi. This indicates a reduced internalization of the toll receptor, +SEM. The data is representative of three independent experiments. Bars 25 μ m.

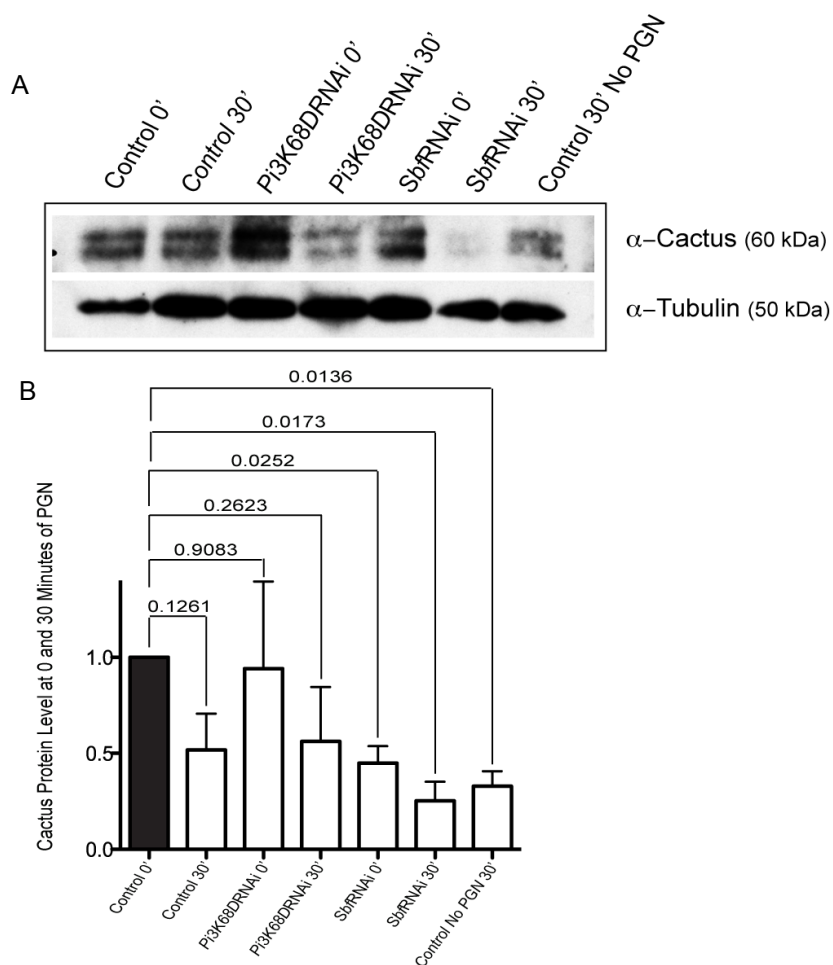


Figure 6: Cactus protein levels decrease after 30 minutes. (A) Cactus protein levels of control, *Pi3K68D* RNAi and *Sbf* RNAi at 0 and 30 minutes of PGN addition. Cactus protein decreased significantly when *Sbf* was knocked down at time 0 and time 30. (B) Cactus protein levels in each lane of the first panel in A are quantified. Normalized Cactus/Tubulin ratio shows significant reduction in Cactus in *Sbf* RNAi at time 0 and time 30. The data is representative of three independent experiments, +SEM.

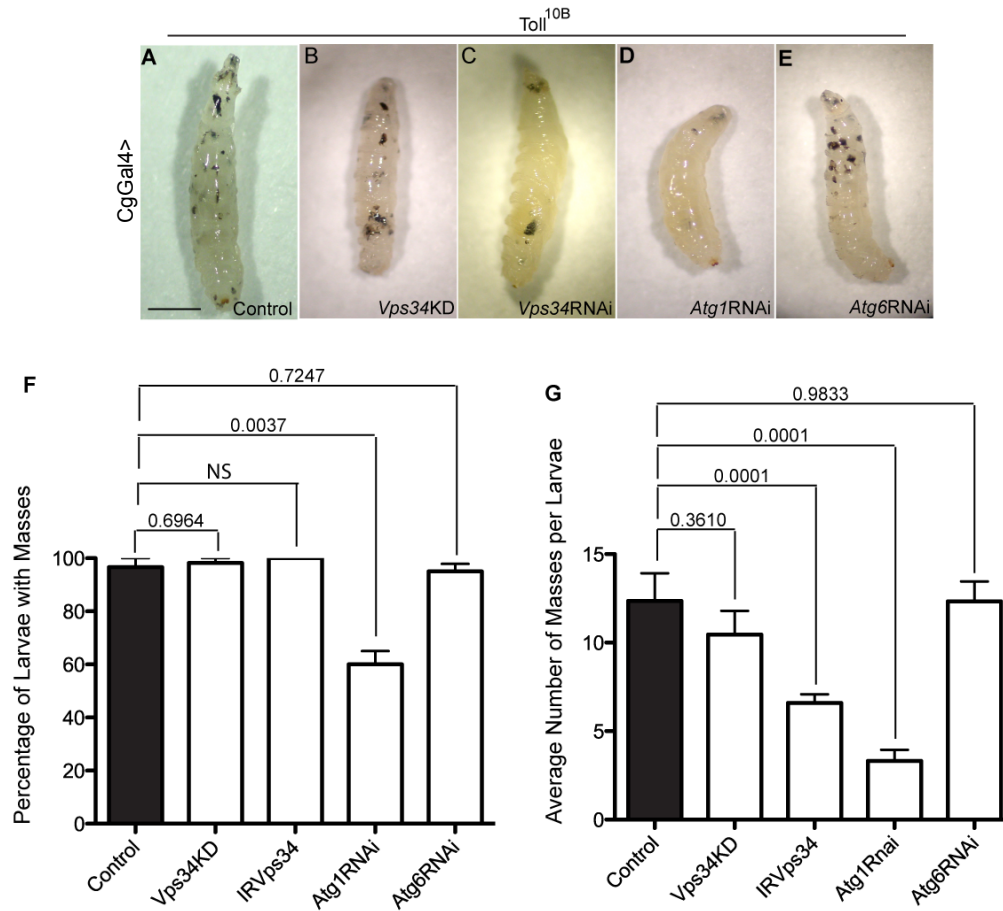


Figure 7: Depletion of *Atg1* suppresses the number and presence of melanotic masses. (A-E) *Drosophila* third instar larvae showing melanotic masses in the different conditions. (A) Control image, over-expression of Toll^{10B} induces melanotic masses. (B) Co-expression of *Vps34*KD, (C) Knockdown of *Vps34*, (D) Knockdown of *Atg1*, (E) Knockdown of *Atg6*. (F) Percentage of larvae with >1 masses per larvae, +SEM. *Atg1* RNAi suppresses the percentage of larvae with >1 masses. (G) Average number of masses per larvae, +SEM. *Vps34* RNAi and *Atg1* RNAi suppress the average number of masses per larvae. The data is representative of three independent experiments. Bars 5 μ m.

DISCUSSION

Previous research had shown that Toll is endocytosed and localizes to the early endosomes (Huang et al. 2010). Additionally, it was shown that Sbf, Pi3K68D, and Rab21 have functions at the early endosomes (Jean et al. 2010). Furthermore, while studying the Sbf complex melanotic masses were discovered. Since the Toll pathway is known to cause tumors upon hyper-activation (Minakhina et al. 2006), the Sbf complex members' interaction with the Toll-signaling pathway was analyzed. Hyper-activated Toll signaling pathway, through the ectopic expression of Toll^{10B}, was used to study the pathway. Hyper-activation of the Toll pathway led to formation of melanotic masses, which were suppressed (Fig 1) when the Sbf complex was knocked down or over-expressed. Although the consequence of over-expression or knockdown was the same, the data suggests a different mechanism through which masses were suppressed. The mass number per larvae and the percentage of larvae with masses decreased when the Sbf complex was over-expressed. However, loss of function led to suppression in mass number only. The masses were observed aggregated together in clumps upon loss of function of the Sbf complex. However, the masses disappeared upon over-expression of the Sbf complex. This suggested that the location of impact was different for the two experiments.

The suppression of melanotic masses indicated a functional interaction between the Sbf complex and Toll-signaling. To address at what level this functional interaction may occur, I took various approaches to test whether the Sbf complex may affect Toll-signaling at the level of the receptor, and specifically, Toll receptor trafficking. I analyzed Toll localization in hemocytes that over-expressed the Sbf complex. Wildtype Toll localized internally when the Sbf complex was over-expressed (Fig 2) and shifted away from the plasma membrane when the complex was knocked down (Fig 4). These results indicated that upon over-expression or knockdown of the Sbf complex Toll localized internally. This was similar to over-expression or knockdown leading to

suppression in mass number. Both experiments had led to the same result. The level of functional interaction remained elusive.

Rab21 is a small GTPase and a member of the Sbf complex. The Sbf complex has been shown to regulate endosomal trafficking (Jean et al. 2012), and therefore its interaction with Toll was studied. Sbf is a GEF for Rab21 and hence activates the small GTPase. From previous data it had been shown that loss of function in *Rab21* leads to melanotic mass formation. In addition, my data indicates that Sbf loss of function leads to a suppression in the number of masses present (Fig 1). Loss and gain of function of the Sbf complex gave a similar result. These two modulations are opposing and, thus, to delineate the cause, additional experiments are required. The different phenotypes of gain or loss of masses observed is possibly due to an alternate mechanism that does not involve the direct relationship of Sbf and Rab21 GEF activity. The balance in P(l)3P/Rab21 regulation is critical, and either an increase or a decrease in this balance leads to the Sbf complex impacting Toll signaling.

To gain a more mechanistic insight I studied uptake of Toll in *Pi3K68D* and *Sbf* depleted conditions. In hemocytes, Toll appeared to be endocytosed normally when *Pi3K68D* was knocked down. However, when *Sbf* was depleted, Toll endocytosis was blocked (Fig 3). This argues for an *Sbf* requirement in Toll endocytosis. This was further strengthened by the results found in *Drosophila* fat body where Toll internalization was also blocked when *Sbf* was knocked down (Fig 5), and Toll was internalized when *Pi3K68D* was depleted. The two results combined show *Sbf* to be important for Toll internalization in different tissues. While *Sbf* was shown to be important, *Pi3K68D*'s function was unclear. Since there was no effect seen with the current knockdown, a stronger knockdown of *Pi3K68D* may help delineate its function. RNAi use leads to a hypomorphic expression, and the protein levels are not entirely depleted. If upon stronger knockdown no change is observed, this may indicate Pi3K68D functions to suppress melanotic masses independent of the Toll internalization step. The function of Pi3K68D could potentially be

subsequent to internalization, and not detected in the experiments. Additional functions of *Pi3K68D* may include maturing Toll endosomes or providing Toll endosomes identity.

To directly assess signaling events downstream of Toll activation, I followed Cactus protein levels, a downstream component of the Toll-signaling pathway. Addition of PGN had been shown to induce Toll signaling in dissected *Drosophila* fat bodies (Bettencourt et al. 2004). However, in my experiments, PGN did not affect cactus protein levels (Fig 6). This result precluded me to understand Sbf complex members' role in the Toll-signaling pathway. Therefore, alternative methods to induce as well as to read-out Toll signaling activity may be necessary. Successful induction of the pathway will allow comparison of signaling in a resting and induced Toll-signaling pathway. For example, laminarin from brown algae cell wall has been used as an inducer in fat body (Bettencourt et al. 2004). In addition, lipoteichoic acid from another gram-positive bacteria, *Bacillus subtilis*, has been used as an inducer (Bettencourt et al. 2004). Furthermore, targets of Toll signaling such as Drosomylin may be measured instead of cactus. Drosomylin is an anti-microbial peptide that is produced upon the addition of Spätzle and subsequent Toll-signaling (Manfruelli, et al. 1999). When the Sbf complex members are depleted, Drosomylin levels will be measured to understand the level of activation. My data suggests that the level of Drosomylin should increase when the larval fat body is induced during *Pi3K68D* depletion, and remain constant during *Sbf* depletion. However, other possibilities depend on how *Pi3K68D* and *Sbf* differentially interact with the Toll pathway. It is possible that they act at two distinct steps in endocytosis or endosomal trafficking that affect signaling. In this scenario induced Drosomylin expression will be impacted. It is also possible that *Pi3K68D* works by different mechanisms downstream or is independent of Toll signaling and target gene expression. *Pi3K68D* may be functioning at a target that is required for mass formation instead.

Given the difference observed between *Pi3K68D* and *Sbf* in the Toll uptake assay, I questioned whether the Toll protein levels were affected by the depletion of the Sbf complex. The

protein levels remained the same and thus are an unlikely cause of uptake difference when *Pi3K68D* or *Sbf* are depleted (Fig 4). Therefore, over-expression studies will be done in both hemocytes and fat body to delineate the reason behind the fact that *Sbf* is required for internalization and *Pi3K68D* is not. Since knockdown of *Sbf* blocks internalization of the Toll receptor, then overexpression of *Sbf* could potentially promote increased Toll internalization. However, since *Pi3K68D* depletion does not lead to a block in uptake, over-expression of *Pi3K68D* may or may not result in a change in the level of internalization. The results may vary from this prediction; however, they could elucidate the function of *Pi3K68D* in relation to Toll-signaling.

The suppression of melanotic masses may have been due to *Sbf* and *Pi3K68D* roles in autophagy. In hyper-activated Toll-signaling conditions, *Toll*^{10B}, I studied the effects of knocking down key autophagic genes on melanotic masses. Knock down of *Atg1* suppressed the number and percentage of masses (Fig 6). This result indicated that *Atg1* is necessary for Toll-induced melanotic mass formation. Knockdown of *Vps34* suppressed the number of melanotic masses but not the presence of masses (Fig 6). *Vps34* is a class III kinases that generates the P(I)3P pool, and assists in the autophagosome formation (Schu et al. 1993; Volinia et al. 1995; and Vergne, et al. 2010). *Vps34* knockdown will lead to a decrease in the P(I)3P pool, and lack of significant amount of P(I)3P turnover may disrupt the endosomal trafficking of Toll. *Atg1* knockdown will lead to a decrease in autophagosome formation, and hence a decrease in autophagy. This step may be critical in the formation of melanotic masses, as the depletion of *Atg1* leads to suppression in both the number and presence of masses. We previously showed that *Atg1* and autophagy are not required for normal hemocyte differentiation or proliferation, but are required for normal hemocyte cell spreading, dispersal and recruitment to wounds (Kadandale et al. 2010). This suggests that cell spreading and dispersal may be key to melanotic mass formation, or alternatively, that autophagy is required in a hemocyte differentiation process that is induced by Toll activation.

Toll signaling pathway interacts with the Sbf complex, as seen by the suppression in the number of melanotic masses when levels of the complex members were altered. In addition, the requirement for *Sbf* in Toll internalization in both hemocytes and fat body is a strong indication that Sbf plays an important role in Toll receptor trafficking. This affect on endocytosis may hinder transduction of Toll-signaling, as one possible basis for how *Sbf* depletion modifies Toll function for mass formation. In addition, a possible function may be during the pinching off of the endocytosing vesicle. Immunogold labeling of Toll protein for electron microscopy analysis of wildtype and *Sbf* depleted cells will indicate the presence or absence of Toll containing endosomal vesicles. This may delineate the exact location of *Sbf* function.

Lastly, hyper-activation of the Jak/Stat pathway leads to the formation of melanotic masses (Minakhina et al. 2006). I have constructed a line that over-expresses constitutively-activated Jak (*hop-TumL* allele). I will deplete specific members of the Sbf complex and measure the effect on melanotic masses. This will further elucidate the specificity of Sbf complex interaction with Toll-signaling.

MATERIALS and METHODS

Fly genetics

Fly stocks were reared at 18°C, or at room temperature. Stocks used include: 1) *w*; *Cg-GAL4*, 2) *w*; *UAS-LacZ*, 3) *w*; *Cg-GAL4*, *UAS-mCherry*, 4) *w*; *UAS-TollGFP*, 5) *w*; *UAS-Toll^{10B}GFP*, 6) *w*; *Cg-GAL4*; *UAS-GFP:Toll/CyO*, 7) *w*; *Cg-GAL4*; *UAS-GFP:Toll^{10B}/CyO*, 8) *w*; *Cg-GAL4*, *UAS-mCherry:Pi3K68D/CyO*, 9) *w*; *Cg-GAL4*, *UAS-mCherry:Sbf*, 10) *w* [1118]; *UAS-IRPi3K68D¹⁶²⁴⁰* 11) *w*; *UAS-IRSbf²²³¹⁷*, 12) *w*; *Cg-Gal4/Cyo*; *Dr/TM6C Sb Tb*, 13) *w*; *UAS-IRVps34¹⁰⁰²⁹⁶*, 14) *w*; *UAS-Vps34KD*, 15) *w*; *UAS-IRAtg1*, 16) *w*; *UAS-IRAtg6²²¹²²*

Melanotic masses quantification

Melanotic masses were quantified from third instar larvae. Larvae were from crosses that were initially incubated at room temperature for 2 days (to allow egg laying), followed by a 3 day incubation at 29° C. Approximately 15 third instar larvae were randomly selected on the 5th day. Larvae were placed in a dish with 1 ml of PBS and examined under a dissecting microscope. The number of melanotic masses per larvae was counted manually. Images of representative larvae were captured for each condition on a Sony Cybershot 3.3 megapixels digital camera (76690) attached to the dissecting microscope. The magnification of the dissection scope was set to 3.2 out of 4 in each respective condition.

Hemocyte dissection and GFP:Toll, and GFP:Toll^{10B} localization analysis

Fly crosses were performed as described above. On the fifth day, third instar larvae were obtained, placed into a silicon chamber attached to a #1.5 coverglass and dissected under a dissecting microscope in 200 µl of PBS. Hemocytes were incubated for 30 minutes at 25° C prior to imaging. This allowed hemocytes to adhere and spread on the cover glass. PBS was replaced with Schneider's complete *Drosophila* media. The samples were analyzed on a Zeiss LSM 700 confocal microscope with a zoom of 1.5X, 5 focal planes were imaged per field.

Anti-Toll uptake analysis

Hemocytes were prepared as for live imaging. After hemocyte spreading, cells were incubated on ice for 60 minutes in 100 μ l of 5 μ g/ml anti-Toll (D300- Santa Cruz) diluted in ice-cold Schneider's media. Cells were washed 3 times with ice-cold Schneider's media. Ice-cold media was replaced with 25°C pre-warmed media to allow uptake. No internalization controls were fixed (4% paraformaldehyde in 1xPBS for 15 minutes at room temperature) right after 25°C media addition. Internalization was allowed for 15 minutes for each respective condition, and was followed by fixation. Cells were blocked in blocking buffer (1X PBS and 10% goat serum) for 15 minutes at room temperature. Non-internalized anti-Toll antibody was detected with a goat anti-rabbit Alexa 488 (1/200 in blocking buffer). After a 1 hour incubation, the non-internalized anti-Toll antibody was blocked with a goat anti-rabbit HRP antibody (1/10 in blocking buffer). After a 1 hour incubation, cells were washed and permeabilized in permeabilization buffer containing (1X PBS with 30% goat serum, and 0.3% Triton X-100). Internalized Toll was detected with a goat anti-rabbit Alexa 546 (1:150 in permeabilization-blocking buffer containing 1X PBS with 30% goat serum and 0.3% Triton X-100). Cells were washed 5 times with 1x PBS and imaged in 1x PBS.

Immunoblot and toll/cactus protein level analysis

S2R⁺ fly cells were used to prepare protein lysates of Toll protein levels analysis. 2.25×10^5 cells were plated in a 12 well plate. Each respective RNAi was added at a concentration of 9-12 μ g/well. After a 45-minute incubation in serum free media, the total volume was brought up to 4 ml with full Schneider's media. After a 72 hour incubation in a 25° C incubator, cells were lysed in lysis buffer (NP-40 1 ml, with 1 μ l of DTT, and 10 μ l of protease inhibitor). This was followed by a 20 minute incubation and a 10 minute centrifugation at 4° C. The supernatant was extracted out. Cell lysates were flash frozen in liquid nitrogen and stored in a -80° C freezer. Samples were run on 3-8% Tris-Acetate Nupage pre-cast gel. Proteins were transferred onto a PVDF membrane, and probed with the appropriate antibodies. Antibodies are anti-Toll (1:1000, d300-Santa Cruz), anti-tubulin (1/2000, Sigma DM1a) anti-Pi3K68D (1:16000, Jean et al), anti-Rab21 (1:5000, Jean

et al), and anti-Sbf (1:8000, Jean et al). Tubulin levels were used to ensure equal protein loading. Three independent experiments were performed and quantified.

Drosophila fat bodies were used to prepare protein lysates for cactus protein level analysis. Fly crosses were done as described above. On the fifth day, third instar larvae were obtained and fat bodies dissected under a dissecting microscope in 200 μ l of full Schneider media (with or without PGN at 10 μ g/ml). Two conditions of 0 or 30 minutes were tested. Fat bodies were lysed in lysis buffer (NP-40 1 ml, with 1 μ l of DTT, and 20 μ l of protease inhibitor) using a mini mortar and pestle, This was followed by a 20 minute incubation on ice and a 10 minute centrifugation at 4° C. The supernatant was extracted out. Fat body protein extracts were flash frozen in liquid nitrogen and stored in a -80° C freezer. Samples were run on 3-8% Tris-Acetate Nupage pre-cast gel. Proteins were transferred onto a PVDF membrane, and probed with the appropriate antibodies. These were cactus (1:100, DHSB), and tubulin (1/2000, Sigma DM1a) antibodies.

Fat body dissection and GFP:Toll localization analysis

Third instar larvae were obtained, as above, and larvae were dissected under a dissecting microscope in 200 μ l of full Schneider media. Dissection was with or without PGN (10 μ g/ml) in two conditions (0 or 30 minutes) before fixation. Larvae carcasses were fixed in 3.7% paraformaldehyde for 15 minutes. Fat body carcasses were transferred in 1x PBS. The next step was to dissect, mount, and image the sample on a LSM 700 confocal microscope.

Confocal microscopy

Live hemocytes were imaged with a 63x magnification (oil immersion), using Zeiss LSM 700 confocal microscope and ZEN software. Fat bodies were imaged with a 40x magnification (oil immersion) using Zeiss LSM 700 confocal microscope and ZEN software.

Analysis methods

Visual analysis was used while detecting the localization of GFP:Toll, and GFP:Toll^{10B} in hemocytes. The respective categories were designated as internal, internal vesicle, external, or diffused. The uptake experiment was quantified using ImageJ software. The freehand selection tool was used to outline individual cells and average signal intensity was used as the indicator of internalization. Fat body localization of GFP:Toll was analyzed with Cell Profiler. The number of puncta normalized per fat body area was used as the indicator of internalization.

Statistical Analysis

Each experiment was repeated at least three times. t-tests were performed using the Prism software and conditions with p-values lower than 0.05 were considered as statistically significant.

REFERENCES

- Abel T, Bhatt R, Maniatis T. (1992). A Drosophila CREB/ATF transcriptional activator binds to both fat body- and liver-specific regulatory elements. *Genes Dev* (3):466-80.
- Anderson KV, Bokla L, Nüsslein-Volhard C. (1985). Establishment of dorsal-ventral polarity in the Drosophila embryo: the induction of polarity by the Toll gene product. *Cell* **42**(3): 791-8.
- Anderson KV. (1998). Pinning down positional information: dorsal-ventral polarity in the Drosophila embryo. *Cell* **95**(4): 439-42.
- Belvin MP, Anderson KV. (1996). A conserved signaling pathway: the Drosophila toll-dorsal pathway. *Annu Rev Cell Dev Biol* **12**: 393-416.
- Bettencourt R, Tanji T, Yagi Y, Ip YT. (2004). Toll and Toll-9 in Drosophila innate immune response. *J Endotoxin Res* **10**(4): 261-8.
- Eskelinen EL, Saftig P. (2009). Autophagy: a lysosomal degradation pathway with a central role in health and disease. *Biochim Biophys Acta* **1793**(4):664-73.
- Fujita K, Maeda D, Xiao Q, Srinivasula SM. (2011). Nrf2-mediated induction of p62 controls Toll-like receptor-4-driven aggresome-like induced structure formation and autophagic degradation. *Proc Natl Acad Sci U S A* **108**(4):1427-32.
- Hu X, Yagi Y, Tanji T, Zhou S, Ip YT. (2004). Multimerization and interaction of Toll and Spätzle in Drosophila. *Proc Natl Acad Sci U S A* **101**(25): 9369-74.
- Huang HR, Chen ZJ, Kunes S, Chang GD, Maniatis T. (2010). Endocytic pathway is required for Drosophila Toll innate immune signaling. *Proc Natl Acad Sci U S A* **107**(18): 8322-7.
- Kadandale P, Kiger AA. (2010). Role of selective autophagy in cellular remodeling: "self-eating" into shape. *Autophagy*. 2010 **6**(8):1194-5.
- Kolter T, Sandhoff K. (2010). Lysosomal degradation of membrane lipids. *FEBS Lett* **584**(9): 1700-12.
- Lemaitre B, Meister M, Govind S, Georgel P, Steward R, Reichhart JM, Hoffmann JA. (1995). Functional analysis and regulation of nuclear import of dorsal during the immune response in Drosophila. *EMBO J* **14**(3): 536-45.
- Lemaitre B, Nicolas E, Michaut L, Reichhart JM, Hoffmann JA. (1996). The dorsoventral regulatory gene cassette spätzle/Toll/cactus controls the potent antifungal response in Drosophila adults. *Cell* **86**(6): 973-83.
- Lodish H, Berk A, Zipursky SL, et al. (2000). Molecular mechanisms of vesicular traffic. *Molecular Cell Biology*. **4**: 17.10.
- Lund VK, DeLotto Y, DeLotto R. (2010). Endocytosis is required for Toll signaling and shaping of the Dorsal/NF-kappaB morphogen gradient during Drosophila embryogenesis. *Proc Natl Acad Sci U S A* **107**(42): 18028-33.
- Luzio JP, Parkinson MD, Gray SR, Bright NA. (2009). The delivery of endocytosed cargo to lysosomes. *Biochem Soc Trans* **37**(Pt 5): 1019-21.

- Macia E, Ehrlich M, Massol R, Boucrot E, Brunner C, Kirchhausen T. (2006). Dynasore, a cell-permeable inhibitor of dynamin. *Dev Cell* **10**(6): 839-50.
- Manfruelli P, Reichhart JM, Steward R, Hoffmann JA, Lemaitre B. (1999). A mosaic analysis in *Drosophila* fat body cells of the control of antimicrobial peptide genes by the Rel proteins Dorsal and DIF. *EMBO J* **18**(12):3380-91.
- McNiven MA. (1998). Dynamin: a molecular motor with pinchase action. *Cell* **94**(2): 151-4.
- Meister M, Lemaitre B, Hoffmann JA. (1997). Antimicrobial peptide defense in *Drosophila*. *Bioessays* **19**(11): 1019-26.
- Meister M, Lagueux M. (2003). *Drosophila* blood cells. *Cell Microbiol* **5**(9):573-80. Review.
- Michel T, Reichhart JM, Hoffmann JA, Royet J. (2001). *Drosophila* Toll is activated by Gram-positive bacteria through a circulating peptidoglycan recognition protein. *Nature* **414**(6865): 756-9.
- Minakhina S, Steward R. (2006). Melanotic mutants in *Drosophila*: pathways and phenotypes. *Genetics* **174**(1): 253-63.
- Nicolas E, Reichhart JM, Hoffmann JA, Lemaitre B. (1998). In vivo regulation of the I κ B homologue cactus during the immune response of *Drosophila*. *J Biol Chem* **273**(17): 10463-9.
- Osterwalder T, Yoon KS, White BH, Keshishian H. (2001). A conditional tissue-specific transgene expression system using inducible GAL4. *Proc Natl Acad Sci U S A* **98**(22):12596-601.
- Puertallano R. (2006). Endocytic trafficking and human disease. *Endosomes* : 119-131.
- Qiu P, Pan PC, Govind S. (1998). A role for the *Drosophila* Toll/Cactus pathway in larval hematopoiesis. *Development* **125**(10): 1909-20.
- Reichhart JM, Georgel P, Meister M, Lemaitre B, Kappler C, Hoffmann JA. (1993). Expression and nuclear translocation of the rel/NF- κ B-related morphogen dorsal during the immune response of *Drosophila*. *C R Acad Sci III* **316**(10): 1218-24.
- Roth S, Stein D, Nüsslein-Volhard C. (1989). A gradient of nuclear localization of the dorsal protein determines dorsoventral pattern in the *Drosophila* embryo. *Cell* **59**(6): 1189-202.
- Rushlow CA, Han K, Manley JL, Levine M. (1989). The graded distribution of the dorsal morphogen is initiated by selective nuclear transport in *Drosophila*. *Cell* **59**(6): 1165-77.
- Russell MR, Nickerson DP, Odorizzi G. (2006). Molecular mechanisms of late endosome morphology, identity and sorting. *Curr Opin Cell Biol* **18**(4): 422-8.
- Schu PV, Takegawa K, Fry MJ, Stack JH, Waterfield MD, Emr SD. (1993). Phosphatidylinositol 3-kinase encoded by yeast VPS34 gene essential for protein sorting. *Science* **260**(5104): 88-91.
- Sever S. (2002). Dynamin and endocytosis. *Curr Opin Cell Biol* **14**(4): 463-7.

- Shen B, Manley JL. (2002). Pelle kinase is activated by autophosphorylation during Toll signaling in *Drosophila*. *Development* **129**(8): 1925-33.
- Silverman N, Paquette N, Aggarwal K. (2009). Specificity and signaling in the *Drosophila* immune response. *Invertebrate Surviv J* **6**(2): 163-174.
- Søndergaard L. (1993). Homology between the mammalian liver and the *Drosophila* fat body. *Trends Genet* **9**(6): 193.
- Steward R. (1989). Relocalization of the dorsal protein from the cytoplasm to the nucleus correlates with its function. *Cell* **59**(6): 1179-88.
- Sun H, Towb P, Chiem DN, Foster BA, Wasserman SA. (2004). Regulated assembly of the Toll signaling complex drives *Drosophila* dorsoventral patterning. *EMBO J* **23**(1): 100-10.
- Takehige K, Baba M, Tsuboi S, Noda T, Ohsumi Y. (1992). Autophagy in yeast demonstrated with proteinase-deficient mutants and conditions for its induction. *J Cell Biol* **119**(2): 301-11.
- Tanji T, Hu X, Weber AN, Ip YT. (2007). Toll and IMD pathways synergistically activate an innate immune response in *Drosophila melanogaster*. *Mol Cell Biol* **27**(12): 4578-88.
- Valanne S, Wang JH, Rämetsä M. (2011). The *Drosophila* Toll signaling pathway. *J Immunol* **186**(2): 649-56.
- Vanlandingham PA, Ceresa BP. (2009). Rab7 regulates late endocytic trafficking downstream of multivesicular body biogenesis and cargo sequestration. *J Biol Chem* **284**(18): 12110-24.
- Vergne I, Deretic V. (2010). The role of PI3P phosphatases in the regulation of autophagy. *FEBS Lett* **584**(7): 1313-8.
- Volinia S, Dhand R, Vanhaesebroeck B, MacDougall LK, Stein R, Zvelebil MJ, Domin J, Panaretou C, Waterfield MD. (1995). A human phosphatidylinositol 3-kinase complex related to the yeast Vps34p-Vps15p protein sorting system. *EMBO J* **14**(14): 3339-48.
- Whalen AM, Steward R. (1993). Dissociation of the dorsal-cactus complex and phosphorylation of the dorsal protein correlate with the nuclear localization of dorsal. *J Cell Biol* **123**(3): 523-34.
- Williams MJ. (2007). *Drosophila* hemopoiesis and cellular immunity. *J Immunol* **178**(8): 4711-6.
- Wu LP, Anderson KV. (1998). Regulated nuclear import of Rel proteins in the *Drosophila* immune response. *Nature* **392**(6671): 93-7.
- Yanagawa S, Lee JS, Ishimoto A. (1998). Identification and characterization of a novel line of *Drosophila* Schneider S2 cells that respond to wingless signaling. *J Biol Chem* **273**(48): 32353-9.